ESC European Society of Cardiology

Cardiovascular Research (2020) **116**, 353–367
doi:10.1093/cvr/cvz139

# Atorvastatin enhances the therapeutic efficacy of mesenchymal stem cells-derived exosomes in acute myocardial infarction via up-regulating long non-coding RNA H19

**Peisen Huang[1,2,3], Li Wang[2,3], Qing Li[1], Xiaqiu Tian[1], Jun Xu[1], Junyan Xu[1], Yuyan Xiong[1], Guihao Chen[1], Haiyan Qian[1], Chen Jin[1], Yuan Yu[1], Ke Cheng[4], Li Qian[2,3]*, and Yuejin Yang[1]***

[1]State Key Laboratory of Cardiovascular Disease, Fuwai Hospital, National Center for Cardiovascular Diseases, Chinese Academy of Medical Sciences and Peking Union Medical College, No.167 Bei Li Shi Road, Xicheng District, Beijing 100037, People's Republic of China; [2]McAllister Heart Institute, University of North Carolina at Chapel Hill, Chapel Hill, NC 27599, USA; [3]Department of Pathology and Laboratory Medicine, University of North Carolina at Chapel Hill, Chapel Hill, NC 27599, USA; and [4]Department of Biomedical Engineering, University of North Carolina at Chapel Hill, North Carolina State University, Chapel Hill and Raleigh, NC 27599, USA

*Received 18 March 2019; revised 9 May 2019; editorial decision 15 May 2019; accepted 16 May 2019; online publish-ahead-of-print 22 May 2019*

**Time for primary review: 20 days**

**Aims** Naturally secreted nanovesicles, known as exosomes, play important roles in stem cell-mediated cardioprotection. We have previously demonstrated that atorvastatin (ATV) pretreatment improved the cardioprotective effects of mesenchymal stem cells (MSCs) in a rat model of acute myocardial infarction (AMI). The aim of this study was to investigate if exosomes derived from ATV-pretreated MSCs exhibit more potent cardioprotective function in a rat model of AMI and if so to explore the underlying mechanisms.

**Methods and results** Exosomes were isolated from control MSCs (MSC-Exo) and ATV-pretreated MSCs ($MSC^{ATV}$-Exo) and were then delivered to endothelial cells and cardiomyocytes *in vitro* under hypoxia and serum deprivation (H/SD) condition or *in vivo* in an acutely infarcted Sprague-Dawley rat heart. Regulatory genes and pathways activated by ATV pretreatment were explored using genomics approaches and functional studies. *In vitro*, $MSC^{ATV}$-Exo accelerated migration, tube-like structure formation, and increased survival of endothelial cells but not cardiomyocytes, whereas the exosomes derived from $MSC^{ATV}$-Exo-treated endothelial cells prevented cardiomyocytes from H/SD-induced apoptosis. In a rat AMI model, $MSC^{ATV}$-Exo resulted in improved recovery in cardiac function, further reduction in infarct size and reduced cardiomyocyte apoptosis compared to MSC-Exo. In addition, $MSC^{ATV}$-Exo promoted angiogenesis and inhibited the elevation of IL-6 and TNF-α in the peri-infarct region. Mechanistically, we identified lncRNA H19 as a mediator of the role of $MSC^{ATV}$-Exo in regulating expression of miR-675 and activation of proangiogenic factor VEGF and intercellular adhesion molecule-1. Consistently, the cardioprotective effects of $MSC^{ATV}$-Exo was abrogated when lncRNA H19 was depleted in the ATV-pretreated MSCs and was mimicked by overexpression of lncRNA H19.

**Conclusion** Exosomes obtained from ATV-pretreated MSCs have significantly enhanced therapeutic efficacy for treatment of AMI possibly through promoting endothelial cell function. LncRNA H19 mediates, at least partially, the cardioprotective roles of $MSC^{ATV}$-Exo in promoting angiogenesis.

* Corresponding author. Tel: +1 919 962 0340; fax: +1 919 966 6012, E-mail: li_qian@med.unc.edu (L.Q.); Tel: +86 10 88398760; fax: +86 10 68351786, E-mail: yangyjfw@126.com (Y.Y.)

**Keywords** Exosomes • Atorvastatin • MSCs • lncRNA H19 • Myocardial infarction

**Graphical Abstract**

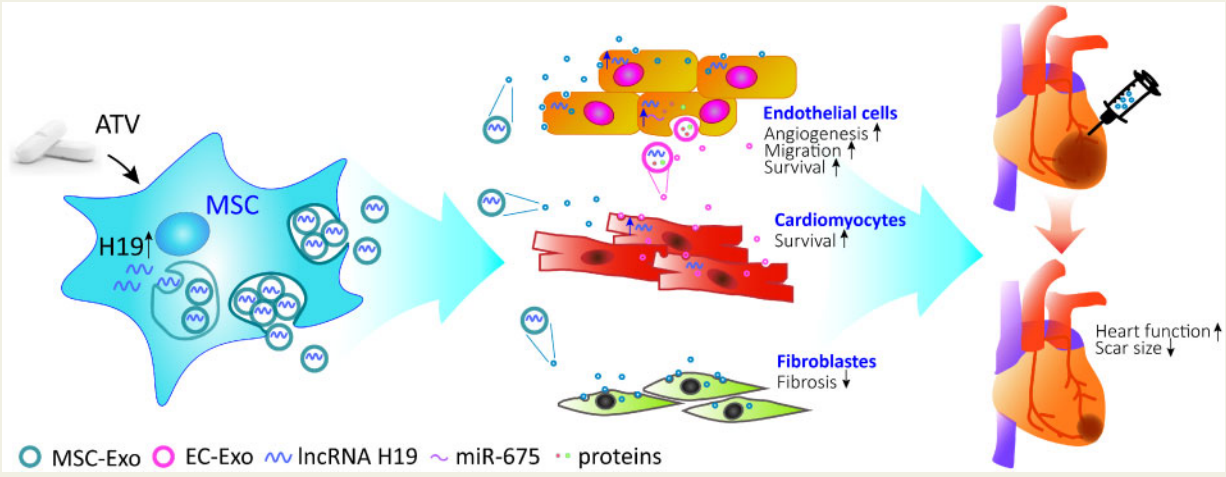


# 1. Introduction

Ischaemic heart disease, including acute myocardial infarction (AMI), is the leading cause of mortality around the world, accounting for 17.3% of all deaths in 2016.[1,2] Stem cells transplantation may be a viable approach to replenish lost cardiomyocytes, promote angiogenesis at the peri-infact region, and reduce adverse remodelling and fibrosis after AMI.[3–5] Among various kinds of stem cells, bone marrow-derived mesenchymal stem cells (MSCs) have accumulated preclinical and clinical evidence to demonstrate their beneficial effects for AMI therapy.[6,7] Mechanistic studies indicated that these beneficial effects are mainly attributed to paracrine effects from secreted factors as opposed to direct muscle regeneration from MSC or MSC-derived cells.[8,9] A large number of growth factors, cytokines, coding, and non-coding RNAs have been implicated in mediating these paracrine effects.[10–12] Exosomes secreted by MSCs carry a complex cargo load of bioactive molecules with the potential to be a novel resource for cardiac regeneration.[13,14] As compared to MSCs, exosomes retain the functionality of their hosts, while conferring several advantages, such as long-term stability, ease of being internalized into recipient cells, minimal immune rejection, and convenient administration.[15] Thus, developing new strategies to optimize such cell-free particles holds great promise for future clinical application.

Exosomes are extracellular, membrane-bound vesicles with a diameter of 30–150 nm, originating intracellularly from a wide array of cell types and transferring their cargo of bioactive molecules between cells.[16] The contents in exosomes would alter when the parent cells are subjected to environmental stimuli,[16–18] which will subsequently influences their biological effects. Previous studies from our group and others have demonstrated that the combined therapeutic benefits with MSCs and atorvastatin (ATV), one of the widely used lipid-lowering drugs for patients with coronary heart disease, significantly improved cardiac function after AMI.[19–21] In addition, ATV pretreatment enhanced the therapeutic potential of MSCs for AMI.[22] Moreover, it has been reported that statins stimulated microglial cell to secret exosomes containing increased insulin-degrading enzyme.[23] Given the potential benefits of using biomimetic exosomes over stem cells themselves for therapeutic purpose,[24,25] it becomes more critical to determine whether ATV pretreatment could affect the exosomal secretion of MSCs and functions of MSC-derived exosomes.

In this study, we investigated the cardioprotective effects of exosomes derived from ATV-pretreated MSCs ($MSC^{ATV}$-Exo) *in vitro* and *in vivo*. $MSC^{ATV}$-Exo significantly improved cardiac function and promoted blood vessel formation compared to exosomes derived from non-pretreated MSCs (MSC-Exo). Cell survival was also profoundly enhanced after $MSC^{ATV}$-Exo treatment. In an effort to explore the underlying molecular mechanism, we found that $MSC^{ATV}$-Exo exhibited a significantly increased level of lncRNA H19 expression. Silencing lncRNA H19 ($MSC^{ATV}$(Si)-Exo) abolished the cardioprotective effects of $MSC^{ATV}$-Exo and overexpression of lncRNA H19 mimicked the improved effects of ATV pretreatment. Our studies therefore suggest that ATV pretreatment can enhance the therapeutic efficacy of MSCs-derived exosomes for myocardial infarction (MI) possibly through enhancing endothelial cell function via a paracrine mechanism. Furthermore, lncRNA H19 seem to mediate the cardioprotective effects of $MSC^{ATV}$-Exo on acutely infarcted hearts.

# 2. Methods

Detailed description of reagents, cell lines, and experimental procedures are available in the Supplementary material online.

## 2.1 Cell isolation, culture, and ATV pretreatment

MSCs were obtained from male Sprague-Dawley (SD) rats (60–80 g). All animal experiments conformed to the NIH guidelines (Guide for the care and use of laboratory animals). Rats were euthanized using $CO_2$ inhalation. After isolation from bone marrow, MSCs cultured in Iscove's Modified Dulbecco's Medium (IMDM, Invitrogen, USA) with 10% foetal bovine serum (FBS, Gibco, USA) in 5% $CO_2$ at 37°C. Passages 3–4

MSCs were pretreated with 1 μmol/L ATV (Sigma, USA) in exosome-free IMDM for 48 h until collection of the conditioned medium. H9C2 myoblasts were cultured in Dulbecco's modified Eagle's medium (DMEM, Invitrogen, USA) with 10% FBS. Human umbilical vein endothelial cells (HUVECs) were cultured in Endothelial Cell Medium (Sciencell, USA) with 5% FBS.

## 2.2 lncRNA H19 siRNA interference and overexpression

For siRNA interference, Lipofectamine 2000 (Invitrogen, USA) and lncRNA H19 siRNA/control siRNA (Genepharma, Shanghai, PRC, http://www.genepharma.com) were mixed and added into Opti-MEM (Invitrogen) according to the manufacturer's instructions and maintained for 10 h. Then the medium was changed to exosome-free IMDM with 1 μmol/L ATV. To build the MSC(H19) cell models (lncRNA H19 overexpressing MSCs), the full-length H19 cDNA and GFP reporter were subcloned into the pHBLV-CMV-MCS-EF1-Zsgreen1-T2A-puro lentiviral vector (Hanbio, Shanghai) and transfected into MSCs and maintained for 10 h to generate MSC(H19). Then, the medium was changed to exosome-free IMDM.

## 2.3 Exosome extraction and identification

Exosomes were isolated by differential centrifugation as previous described.[26] In brief, the conditioned supernatant of MSCs pretreated or non-pretreated with ATV, or interfered by lncRNA H19 siRNA were collected and centrifuged. After removing dead cells, cell debris, and large extracellular vesicles, exosomes were isolated by repeated ultracentrifugation and resuspended in PBS. Exosomes were identified by transmission electron microscope (TEM, HITACHI, H-600IV, Japan), Nanoparticle Tracking Analysis (NTA, Malvern Instruments, UK) and western blot.

## 2.4 *In vitro* functional assays

A Matrigel tube-formation assay and scratch assay were performed to assess *in vitro* angiogenesis and migration of HUVECs after the cells were treated with different exosomes. The apoptosis of HUVECs and H9C2 myoblasts were induced by hypoxia and serum deprivation (H/SD) condition, and evaluated by flow cytometry assay after Annexin V/propidium iodide (PI) staining.

## 2.5 Co-culture experiment

For co-culture experiment, we seeded HUVECs with EBM-2 medium in the Transwell inserts and once cultures reached 70–80% confluence we added PBS, MSC-Exo or $MSC^{ATV}$-Exo (2 μg/mL) with or without 20 μM GW4869 treatment for 12 h. After that we cultured H9C2 in 24-well plates and once reached 70–80% confluence immediately the inserts with HUVECs or controls were placed onto the H9C2 wells. After 12 h incubation, the cells were put in H/SD condition for 12 h, and evaluated by flow cytometry assay after Annexin V/propidium iodide (PI) staining.

## 2.6 MI model induction and exosome delivery

Animal protocols were performed with approval of the Experimental Animals Ethics Committee of Fuwai Hospital and all procedures conformed to the NIH guidelines. Animals were randomized into different treatment groups. All surgeries and subsequent analyses were performed in a blinded fashion for intervention. Female SD rats (200–220 g weight) were anaesthetized by intraperitoneal injection of 100 mg/kg ketamine combined with 10 mg/kg xylazine and ventilated via tracheal intubations connected to a rodent ventilator. MI was induced by ligation of left anterior descending coronary artery as previously described.[22,27] Exosomes (10 μg, in 100 μL PBS) or PBS were injected into the border zone of infarcted heart at three sites. Transthoracic two-dimensional M-mode echocardiography was performed at baseline and at 3, 7, and 28 days post-surgery using Vevo 2000 high-resolution micro imaging system (Visual Sonic) after rats were anaesthetized with isoflurane. Left ventricular ejection fraction (LVEF), fractional shortening (FS), left ventricular end-diastolic volume (LVEDV), and left ventricular end-systolic volume (LVESV) were measured and calculated as previously described.[22,27]

## 2.7 Histological analysis

All rats were sacrificed after endpoint echocardiography measurements being recorded. Masson's Trichrome stain and Sirius Red stain were used to quantify the extent of fibrosis and infarct size in left ventricle. Haematoxylin-Eosin (HE) stain was used to evaluate the degree of inflammatory cell infiltration. At least three sections from each heart were stained. Blood vessel density was assessed and quantified using immunofluorescence of CD31 and α-SMA as described in Supplementary material online, *Methods*. The number of apoptotic cells and senescent cells in the tissue sections was counted by terminal deoxynucleotidyl transferase dUTP nick end labelling (TUNEL) assay, Cleaved Caspase-3 staining and $p16^{Ink4a}$ staining. H19+ cells in hearts sections were labelled with a lncRNA-H19 probe (green, 5'-FAM-CCUUUGCUAACUGUCCUGCCUUUCUAUGUGCCAUUCUG-3') using Fluorescent in site hybridization (FISH). Nucleus were counterstained with 4', 6-diamidino-2-phenylindole (DAPI). The number of positive cells in the field was quantified.

## 2.8 Exosomal lncRNA sequencing

The lncRNA sequencing was performed in both MSC-Exo and $MSC^{ATV}$-Exo. Differentially expressed lncRNAs were identified through fold change >1.5 and Q value <0.001 with the threshold set for up- and down-regulated genes. lncRNA sequencing data have been deposited in NCBI's Gene Expression Omnibus under accession code GSE113570 (https://www.ncbi.nlm.nih.gov/geo/query/acc.cgi?acc=GSE113570).

## 2.9 Statistical analysis

Data were displayed with mean ± standard error of mean (SEM) on a bar or scatter dot plot (each dot represents one animal or independent experiment). Continuous variables were compared by the Student's *t*-test. Comparison of more than two groups was performed by one-way analysis of variance (ANOVA). Data were analysed with SPSS 22 (IBM) or GraphPad Prism 7 for Windows, version 7.01 (GraphPad Software, Inc.). Graphs were assembled in GraphPad Prism 7. A *P*-value <0.05 was considered significant.

# 3. Results

## 3.1 Characterization of exosomes derived from MSCs

MSCs were isolated from bone marrow of SD rats. MSCs at Passages 3–4 were typically spindle shaped and adherent to the plastic dishes. There was no significant difference in morphology of MSCs with or without

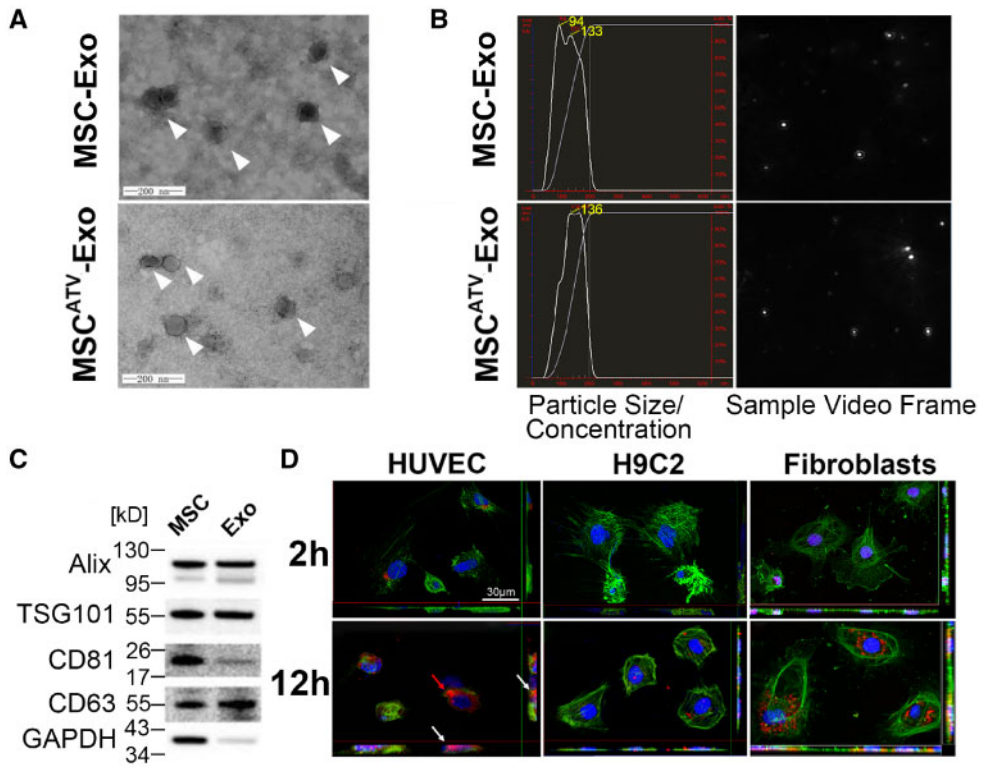


**Figure 1** Characterization and functional validation of exosomes derived from ATV-treated MSCs. (*A*) Cup-shaped morphology of purified MSC-Exo and MSC$^{ATV}$-Exo (arrowhead) assessed by TEM. (*B*) The particle size, particle concentration, and video frame of MSC-Exo and MSC$^{ATV}$-Exo were analysed by nanoparticle tracking analysis. There were no significant differences between MSC-Exo and MSC$^{ATV}$-Exo. (*C*) Representative images of western blot showing the exosomal protein markers. (*D*) Representative confocal images showing that red fluorescence dye PKH26 labelled exosomes were endocytosed by HUVECs, H9C2s, and cardiac fibroblasts after 2 and 12 h incubation. (*A–D*) $n = 5$.

treatment of ATV for 24 h (Supplementary material online, *Figure S1A*). The identity of the MSCs were further confirmed by staining for the canonical surface markers probing as CD90+ CD29+ CD45- CD11- (Supplementary material online, *Figure S1B*).

Transmission electron microscopy (TEM) imaging analysis demonstrated that exosomes from ATV-pretreated MSCs morphologically resembled a typical cup-shaped structure and were around 100 nm in size (*Figure 1A*). NTA was performed to characterize the size distribution of exosomes (*Figure 1B*). The particle size and concentration were similar between MSC-Exo and MSC$^{ATV}$-Exo (*Figure 1A* and *B*). Western blot analyses showed that exosomes were positive for the exosome-specific markers Alix, TSG101, CD81, and CD63 (*Figure 1C*). To evaluate the internalization of MSC$^{ATV}$-Exo by cardiovascular cells, we pre-labelled the exosomes with PKH26 (a red fluorescent cell linker for general cell membrane labelling) and added theses exosomes to cultured recipient cells, including endothelial cells (ECs), cardiomyocytes (CMs), and cardiac fibroblasts. Confocal images taken at 2 and 12 h after exosome addition showed that HUVECs efficiently internalized exosomes at 2 h after incubation and uptaked significant amount of labelled exosomes by Hour 12 (*Figure 1D*, left panel). However, minimal PKH26+ exosomes could be detected in CMs and fibroblasts during the first 2 h. By Hour 12, whereas exosome uptake by the CMs were still minimal, most fibroblasts internalized detectable amount of PKH26+ exosomes (*Figure 1D*, middle and right panels). These data demonstrated that ECs and cardiac fibroblasts more efficiently internalize MSC-derived exosomes than CMs.

## 3.2 MSC$^{ATV}$-Exo enhances tube formation, migration, and survival of endothelial cell

Promoting neovascularization is one of the well-documented mechanisms underlying the therapeutic benefits conferred by stem cell-derived exosomes. To assess the optimal dosage of exosomes, different concentrations of MSC$^{ATV}$-Exo were applied to HUVECs to evaluate their ability to promote vessel formation and EC migration. Treatment of exosomes at a concentration of 0–2 μg/mL resulted in a dose-dependent increase in the total length of tubes and migration rates. Instead, no significant difference was observed when MSC$^{ATV}$-Exo was applied between 2 and 4 μg/mL (*Figure 2A* and *B*; Supplementary material online, *Figure S2*). Thus, we used the concentration of 2 μg/mL for the following in *vitro* assays.

Consistent with previously published, our control MSC-derived exosomes (MSC-Exo) promoted vessels formation of HUVECs. Importantly, treatment with MSC$^{ATV}$-Exo further promoted HUVEC tubulogenesis, compared to MSC-Exo and MSC$^{ATV}$-Exo with ruptured membranes by exposing to ultrasound [MSC$^{ATV}$-Exo (Ultra), *Figure 2C* and *D*]. Consistently, the migration distance of the HUVECs treated with MSC$^{ATV}$-Exo was significantly greater compared to that of the HUVECs treated with MSC-Exo or MSC$^{ATV}$-Exo (Ultra) (*Figure 2E* and *F*). MSC-derived exosomes also protected HUVECs from apoptosis caused by H/SD. A significant reduction in apoptosis was observed in MSC$^{ATV}$-Exo group compared with MSC-Exo and MSC$^{ATV}$-Exo (Ultra) group (*Figure 2G–J*). These data suggested that MSC$^{ATV}$-Exo exhibited

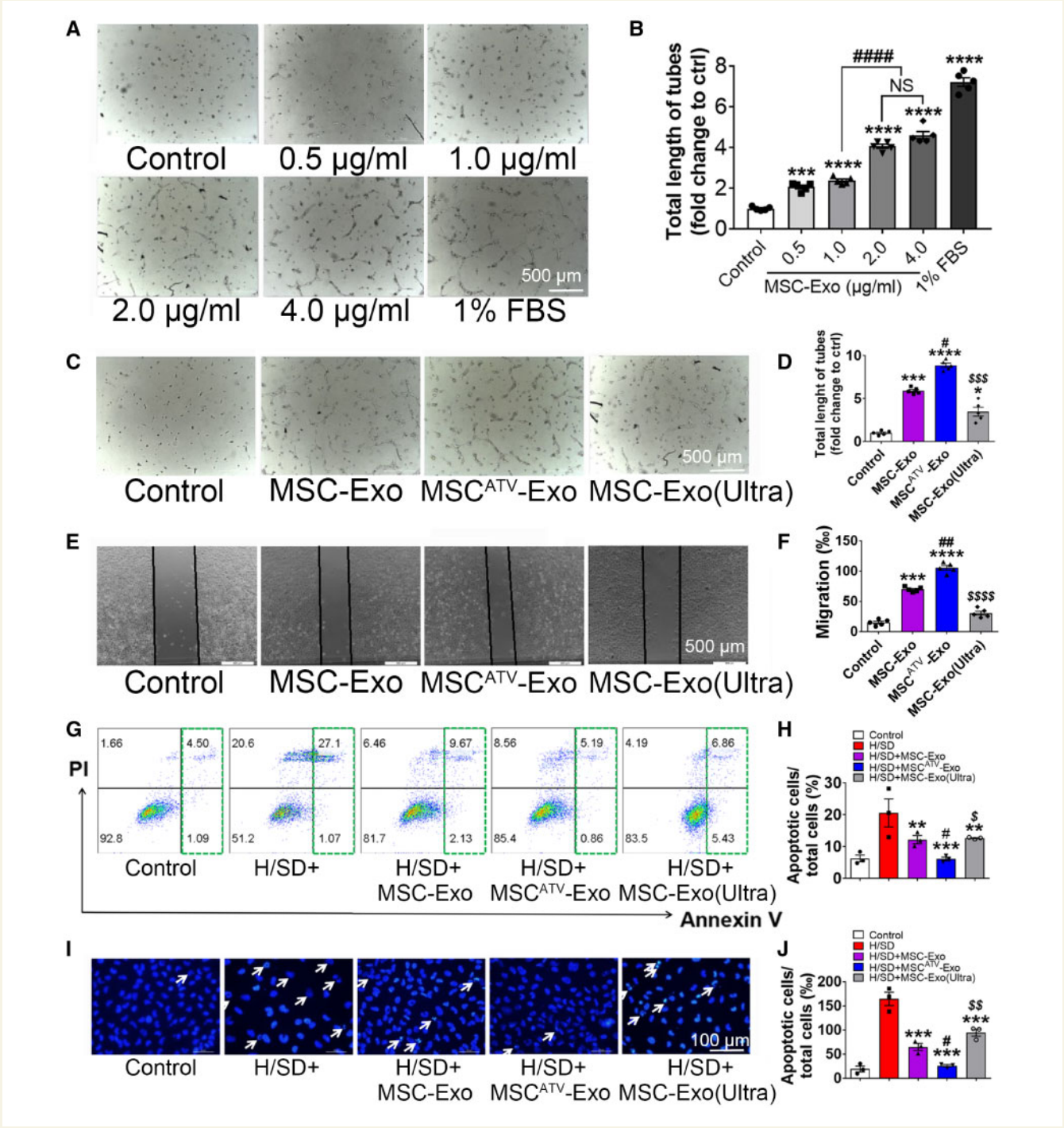


**Figure 2** MSC$^{ATV}$-Exo promoted capillary like tubes formation, migration, and survive of HUVECs. (*A–D*) Capillary-like tube formation assay on Matrigel was assessed 6 h after HUVECs seeding with FBS free medium supplemented with exosomes. (*A*) Representative images showing tube formation in HUVECs treated with different concentration of MSC-Exo. Scale bar = 500 μm. (*B*) Quantification of tube length in each concentration group ($n = 5$). (*C*) Representative images showing tube formation in HUVECs treated with PBS, MSC-Exo, MSC$^{ATV}$-Exo, or MSC-Exo (Ultra). (*D*) Quantification of tube length in each type of exosome group ($n = 5$). (*E* and *F*) HUVECs migration was monitored 12 h after the scratch in HUVEC maintained in no FBS medium supplemented with exosomes (*E*) and quantitative data (*F*). Scale bar = 500 μm. (*G–J*) Flow cytometry assay and Hoechst 33342 nucleic acid stain for apoptosis of HUVECs after treated with PBS, MSC-Exo, MSC$^{ATV}$-Exo, or MSC-Exo (Ultra) and exposed to H/SD. (*G*) Scatter diagram of apoptosis in HUVECs treated with exosomes and negative control. (*H*) Histogram of apoptosis events in different groups ($n = 3$). (*I*) Representative images of Hoechst 33342 nucleic acid stain. Arrows point cells that are apoptotic cells. Scale bar = 100 μm. (*J*) Quantification of apoptosis cells in each group ($n = 3$). All data are mean ± SEM. Statistical analysis was performed with one-way ANOVA followed by Tukey's test. $^{**}P < 0.01$, $^{***}P < 0.001$, $^{****}P < 0.0001$ vs. Control or H/SD group; $^{\#}P < 0.05$, $^{\#\#}P < 0.01$ vs. MSC-Exo group; $^{\$}P < 0.05$, $^{\$\$}P < 0.01$, $^{\$\$\$}P < 0.001$, and $^{\$\$\$\$}P < 0.0001$ vs. MSC$^{ATV}$-Exo group. NS, not significant.

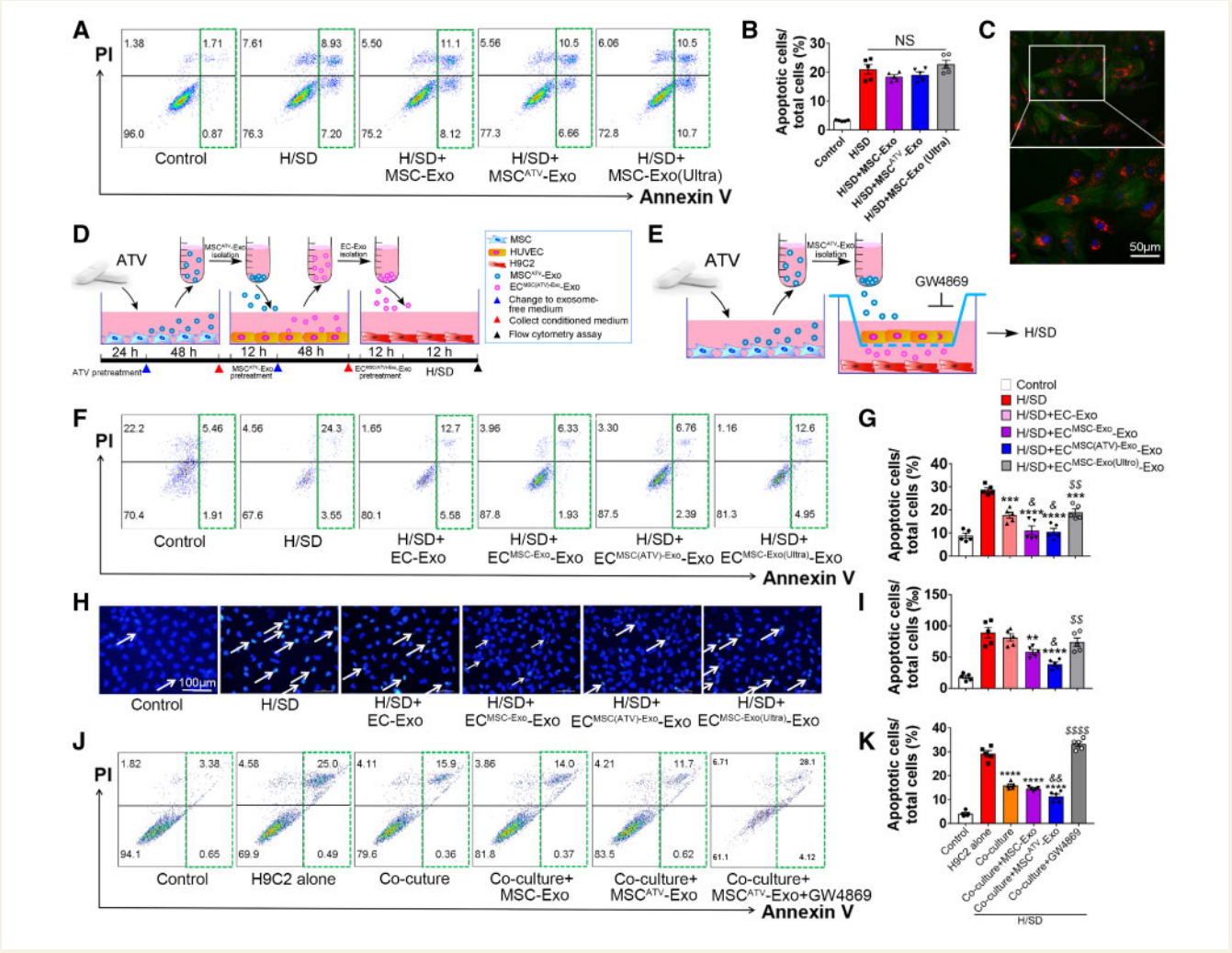


**Figure 3** MSC$^{ATV}$-Exo enhanced the survival of H9C2 cardiomyocytes under H/SD conditions mediated by exosomes derived from endothelial cell. (*A*, *B*) Representative images and quantification of flow cytometry assay for apoptosis in H9C2 cardiomyocytes after treated with PBS (Control), MSC-Exo, MSC$^{ATV}$-Exo or MSC-Exo (Ultra), and H/SD. ($n = 5$). (*C*) Representative immunofluorescent images showing that red fluorescence dye PKH26 labelled HUVEC-derived exosomes were endocytosed by H9C2 cardiomyocytes after 12 h incubation. (*D*) Schematic of the EC-Exo-mediated H9C2 cells protection experiment. (*E*) Schematic of the co-culture HUVECs with H9C2 cardiomyocytes experiment by using Transwell system. (*F–I*) Flow cytometry assay and Hoechst 33342 nucleic acid stain for apoptosis of H9C2 cardiomyocytes after treated with exosome derived from MSC-Exo, MSC$^{ATV}$-Exo or MSC-Exo (Ultra) pretreating HUVECs. (*F*) Scatter diagram of apoptosis in H9C2 treated with different types of EC-Exo and negative control and quantitative data (*G*, $n = 5$). (*H*) Representative images of Hoechst 33342 nucleic acid stain and quantitative data (*I*, $n = 5$). Arrows point cells that are apoptotic cells. Scale bar = 100 μm. (*J*) Flow cytometry assay for apoptosis of H9C2 cardiomyocytes after co-cultured with MSC-Exo or MSC$^{ATV}$-Exo-pretreated HUVECs with or without adding GW4869. (*K*) Quantitative data of J ($n = 5$). All data are mean ± SEM. Statistical analysis was performed with one-way ANOVA followed by Tukey's test. $^{**}P < 0.01$, $^{***}P < 0.001$, $^{****}P < 0.0001$ vs. H/SD group; $^{\&}P < 0.05$, $^{\&\&}P < 0.01$ vs. H/SD+EC-Exo group or co-culture group; $^{\$\$}P < 0.01$, $^{\$\$\$\$}P < 0.0001$ vs. H/SD+EC$^{MSCATV\text{-}Exo}$-Exo group. NS, not significant.

more significant protective effect on ECs than MSC-Exo under *in vitro* conditions we have tested so far.

## 3.3 MSC$^{ATV}$-Exo protected CMs from apoptosis under H/SD mediated by endothelial cell-derived exosomes

To investigate the biologic effects of MSC$^{ATV}$-Exo on CMs, H9C2 cardiomyocytes were treated with MSC-Exo, MSC$^{ATV}$-Exo or MSC$^{ATV}$-Exo (Ultra) and then subjected to H/SD. No significant difference was found among the groups (*Figure 3A* and *B*). Hoechst 33342 staining also showed no significant difference (Supplementary material online, *Figure S3*).

As ECs demonstrated significantly more efficient MSC-derived exosomes uptake capacity than CMs, we wanted to investigate whether ECs could relay the protective effect of MSC$^{ATV}$-Exo on CMs. To this end, we first detected the efficiency of CMs uptaking ECs derived exosomes and found that H9C2 cardiomyocytes can efficiently uptake the PKH26 labelled HUVEC-Exo in 12 h compared with MSC-Exo (*Figure 3C*). We then incubated HUVECs with the aforementioned three types of MSC-derived exosomes and PBS, respectively, for 12 h before further culturing the cells on exosome-free Endothelium Cell Medium with 5% FBS for an additional 24 h. Subsequently, the conditional medium was collected to isolate exosomes secreted by PBS, MSC-Exo, MSC$^{ATV}$-Exo, or MSC$^{ATV}$-Exo (Ultra)

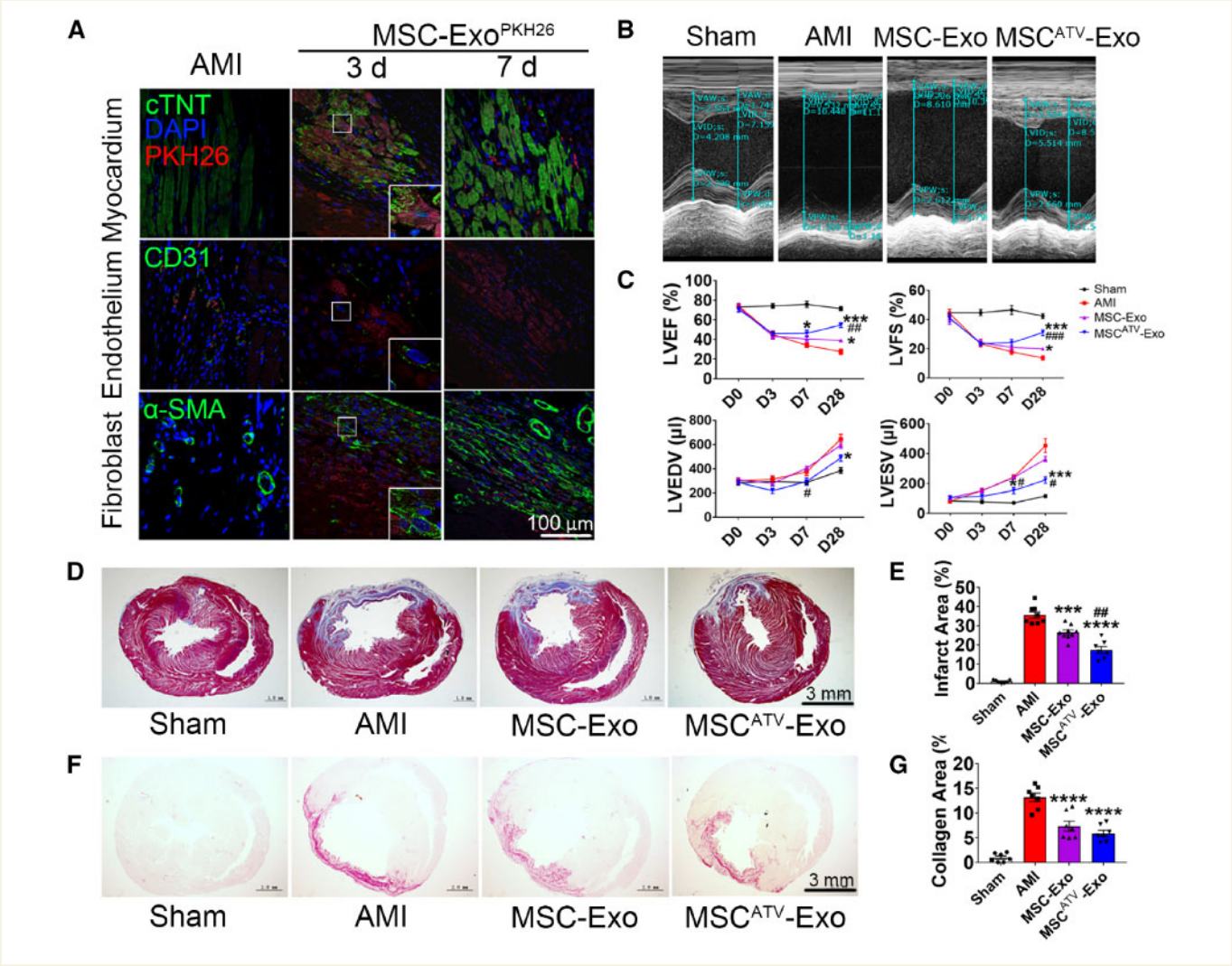


**Figure 4** MSC$^{ATV}$-Exo improved cardiac function and ameliorated fibrosis after MI. (*A*) Distribution of MSC$^{ATV}$-Exo pre-labelled with PKH26 in the infarcted heart on Day 3 and Day 7 post-injection. Scale bar = 100 μm. (*B*) Representative echocardiogram of rat heart in different groups at 28 days post-MI. (*C*) Significantly enhanced LVEF, LVFS, LVEDV, and LVESV in rats transplanted with MSC$^{ATV}$-Exo compared with other groups ($n$ = 8–10 for each group). (*D*) Representative transverse heart sections analysed with Masson Trichrome staining at 4 weeks after MI. Red, myocardium; blue, scarred fibrosis. Scale bar = 3 mm. (*E*) Quantitative data for the LV fibrotic area ($n$ = 7–9 for each group). (*F*) Representative Sirius Red staining images for collagen analyse in each group and the quantitative data (*G*) ($n$ = 7–9 for each group). Scale bar = 3 mm. All data are mean ± SEM. Statistical analysis was performed with one-way ANOVA followed by Tukey's test. *$P$ < 0.05, **$P$ < 0.01, ***$P$ < 0.001, ****$P$ < 0.0001 vs. AMI group; $^{\#\#}P$ < 0.01, $^{\#\#\#}P$ < 0.001 vs. MSC-Exo group.

pretreated HUVECs (named as EC-Exo, EC$^{MSC\text{-}Exo}$-Exo, EC$^{MSCATV\text{-}Exo}$-Exo, and EC$^{MSC\text{-}Exo(Ultra)}$-Exo, respectively). CMs were then treated with EC-derived exosomes and exposed under H/SD condition to induce cell apoptosis (*Figure 3D*). Flow analyses showed that the H/SD + EC$^{MSC\text{-}Exo}$-Exo and EC$^{MSCATV\text{-}Exo}$-Exo groups demonstrated a significant reduction in apoptosis compared to the H/SD, H/SD + EC-Exo, and EC$^{MSC\text{-}Exo(Ultra)}$-Exo groups (*Figure 3F* and *G*). Similar result was observed using Hoechst 33342 staining assay (*Figure 3H* and *I*). These results indicated that exosomes derived from MSC$^{ATV}$-Exo pretreated ECs significantly improved the survival of the CMs subjected to H/SD.

Moreover, we performed a co-culture experiment to confirm this transfer effect of EC-Exo to protect H9C2 from H/SD. We co-cultured H9C2 with HUVECs and tested the beneficial effects of MSC-Exo with or without GW4869, an exosome secretion inhibitor (*Figure 3E*).[28] After 12 h incubation under H/SD, we observed a huge decrease in apoptosis when H9C2 were co-cultured with HUVECs compared to H9C2 alone group (*Figure 3J* and *K*). In addition, MSC$^{ATV}$-Exo treatment further reduced the apoptosis of H9C2 when co-culture with HUVECs. Nevertheless, when HUVECs were pre-incubated with GW4869, the percentage of apoptotic H9C2 cardiomyocytes was increased dramatically (*Figure 3J* and *K*). Taken together, ECs can act as a mediator of the protective benefit of MSC$^{ATV}$-Exo on CMs through uptaking MSCs-derived exosomes and secreting exosomes which in turn supports cardiomyocyte survival under H/SD.

## 3.4 MSC$^{ATV}$-Exo effectively preserved cardiac function in a rat MI model

To assess the beneficial potential of exosomes *in vivo*, MSC-Exo, MSC$^{ATV}$-Exo or PBS (AMI control group) were intramyocardially

**Table 1 Haemodynamics, cardiac performance, and infarct size data of rat AMI models at 4-week post-infarction**

| | Sham | AMI | MSC-Exo | $MSC^{ATV}$-Exo |
|---|---|---|---|---|
| LVEDP (mmHg) | 11.68 ± 2.76 | 16.55 ± 7.18 | 15.62 ± 1.74 | 13.06 ± 1.69* |
| Max *dP/dt* (mmHg/s) | 7113.36 ± 488.63 | 6054.66 ± 512.57 | 6734.11 ± 582.16 | 7672.66 ± 1979.56 |
| Min *dP/dt* (mmHg/s) | -5974.45 ± 228.14 | -3866.98 ± 261.84 | -4776.72 ± 481.86 | -5461.53 ± 1105.89* |
| LVEF (%) | 71.50 ± 2.06 | 27.52 ± 2.75 | 39.17 ± 1.31* | 54.75 ± 2.50*** |
| LVFS (%) | 42.39 ± 1.65 | 13.69 ± 1.48 | 20.00 ± 0.80* | 31.07 ± 2.07*** |
| LVEDV (μL) | 384.60 ± 23.88 | 644.94 ± 39.83 | 594.47 ± 25.89 | 489.44 ± 25.57* |
| LVESV (μL) | 115.58 ± 10.21 | 453.54 ± 45.87 | 363.16 ± 16.39 | 224.05 ± 23.36*** |
| Infarct area (%) | 0.95 ± 0.30 | 35.60 ± 1.67 | 26.53 ± 1.25*** | 17.41 ± 1.79**** |
| Collagen area (%) | 0.99 ± 0.33 | 13.18 ± 0.87 | 7.35 ± 1.01**** | 5.89 ± 0.62**** |

$n = 7–9$ for each group. All data are mean ± SEM. Statistical analysis was performed with one-way ANOVA followed by the Tukey's test.
LVEDP, left ventricular end-diastolic pressure.
*$P < 0.05$.
***$P < 0.001$.
****$P < 0.0001$ compared with AMI group.

injected into the border zone of infarcted rat hearts 30 min after injury. Distribution of PKH26-labelled $MSC^{ATV}$-Exo (Exo-PKH26) in infarcted heart was monitored on Day 3 and Day 7 after injury. Large areas positive for Exo-PKH26 can be detected in the myocardium, around the endothelium and fibroblast cells on Day 3 after MI. On Day 7, minimal red fluorescent spots were detected (*Figure 4A*). Echocardiography revealed that injection of $MSC^{ATV}$-Exo mitigated MI-induced left ventricular (LV) dilation (*Figure 4B*). Though on Day 7 after MI the $MSC^{ATV}$-Exo group showed a moderate yet not statistically significant enhancement in LVEF compared to the AMI group, the improvement of LVEF and LVFS by MSC-Exo or $MSC^{ATV}$-Exo were highly significant on Day 28 post-MI. In addition, $MSC^{ATV}$-Exo demonstrated a therapeutic superiority to MSC-Exo in systolic function improvement (*Figure 4C*). Between the MSC-Exo and $MSC^{ATV}$-Exo groups, $MSC^{ATV}$-Exo treatment moderately decreased LVEDV and LVESV of infarcted heart compared to MSC-Exo group at 7 and 28 days after MI (*Figure 4C*). Haemodynamic data at 4 weeks after AMI showed that left ventricular end-diastolic pressure (LVEDP) was also lower in $MSC^{ATV}$-Exo group (*Table 1*). Histological analysis indicated significantly decreased scar size in $MSC^{ATV}$-Exo group (17.41 ± 4.74%) compared to AMI (35.60 ± 4.73%) and MSC-Exo groups (26.53 ± 3.75%) (*Figure 4D* and *E*). Collagen area also decreased significantly in $MSC^{ATV}$-Exo group compared to other groups (*Figure 4F* and *G*). These results suggested that ATV pretreatment significantly promoted the beneficial effects of MSC-derived exosomes on functional recovery of infarcted hearts.

## 3.5 $MSC^{ATV}$-Exo promoted angiogenesis and cardiomyocyte survival in MI hearts

To uncover the mechanism underlying the augmented cardiac function conferred by exosomal therapy on MI hearts, we performed immunofluorescence using antibodies against α-SMA and CD31 to stain arteriole and capillary. Arteriole density was significantly increased in the $MSC^{ATV}$-Exo group compared to MSC-Exo and AMI groups 4 weeks after infarction (*Figure 5A* and *B*). Similar trends were observed in capillary density (*Figure 5A* and *B*).

To explore the anti-apoptotic effect of exosomes on myocardial cells, TUNEL and Cleaved Caspase-3 staining was performed on 4 weeks MI hearts. The number of apoptotic cells was significantly reduced in the myocardial boarder zone treated with different exosomes compared to that treated with PBS. Importantly, the $MSC^{ATV}$-Exo group was found to have the lowest number of TUNEL+ (*Figure 5A* and *B*) and Cleaved Caspase-3+ cells (*Figure 5C* and *D*). These results indicate that the $MSC^{ATV}$-Exo led to enhanced angiogenesis and increased cell survival which may contribute to the enhanced cardiac reparative ability.

## 3.6 $MSC^{ATV}$-Exo decreased inflammation and fibrosis genes expression

Inflammation and subsequent fibrosis are important pathological reactions during the formation of scar post-MI. We, therefore, assessed the degree of inflammation in the infarcted hearts using HE staining. We observed decreased infiltration of inflammatory cells in the $MSC^{ATV}$-Exo group compared to other groups (*Figure 5E*). Furthermore, 3 days after exosome delivery cytokines such as IL-6 and TNF-α were decreased in the $MSC^{ATV}$-Exo group compared to others (*Figure 5F* and *G*).

We then investigated whether $MSC^{ATV}$-Exo could alter the expression of fibrosis-related genes *in vitro*. We found that the expression level of Col1a1 and Col3a1 in cardiac fibroblasts was significantly down-regulated after treatment with $MSC^{ATV}$-Exo compared to TGF-β and TGF-β + MSC-Exo groups (Supplementary material online,*Figure S4*). As intrinsic cardiac aging is considered to highly influence the pathogenesis of cardiovascular disease and regeneration,[29,30] we also investigated the level of cellular senescence in the hearts after exosomes therapy by $p16^{Ink4a}$ staining, a senescence biomarker also known as Cdkn2a.[31] Remarkably, a significant increase of senescent cells (4–8%) was found in all of the infarcted groups compared with Sham group. However, no significant difference was found after exosomes therapy (Supplementary material online,*Figure S5*). Taken together, the exhibited enhanced therapeutic effects of $MSC^{ATV}$-Exo may be partly attributable to its role in suppression of inflammation and fibrosis genes.

## 3.7 ATV pretreatment increased MSCs lncRNA H19 expression and its release via exosomes

Accumulating evidence showed that lncRNAs loaded in exosomes play an important role in executing their cellular function.[32–34] In order to investigate the molecular mechanisms underlying the further enhancement of $MSC^{ATV}$-Exo in cardiac protection, we performed lncRNA sequencing on exosomes secreted from $MSC^{ATV}$ and MSC to identify differentially expressed lncRNA. The molecule size range of RNA samples from

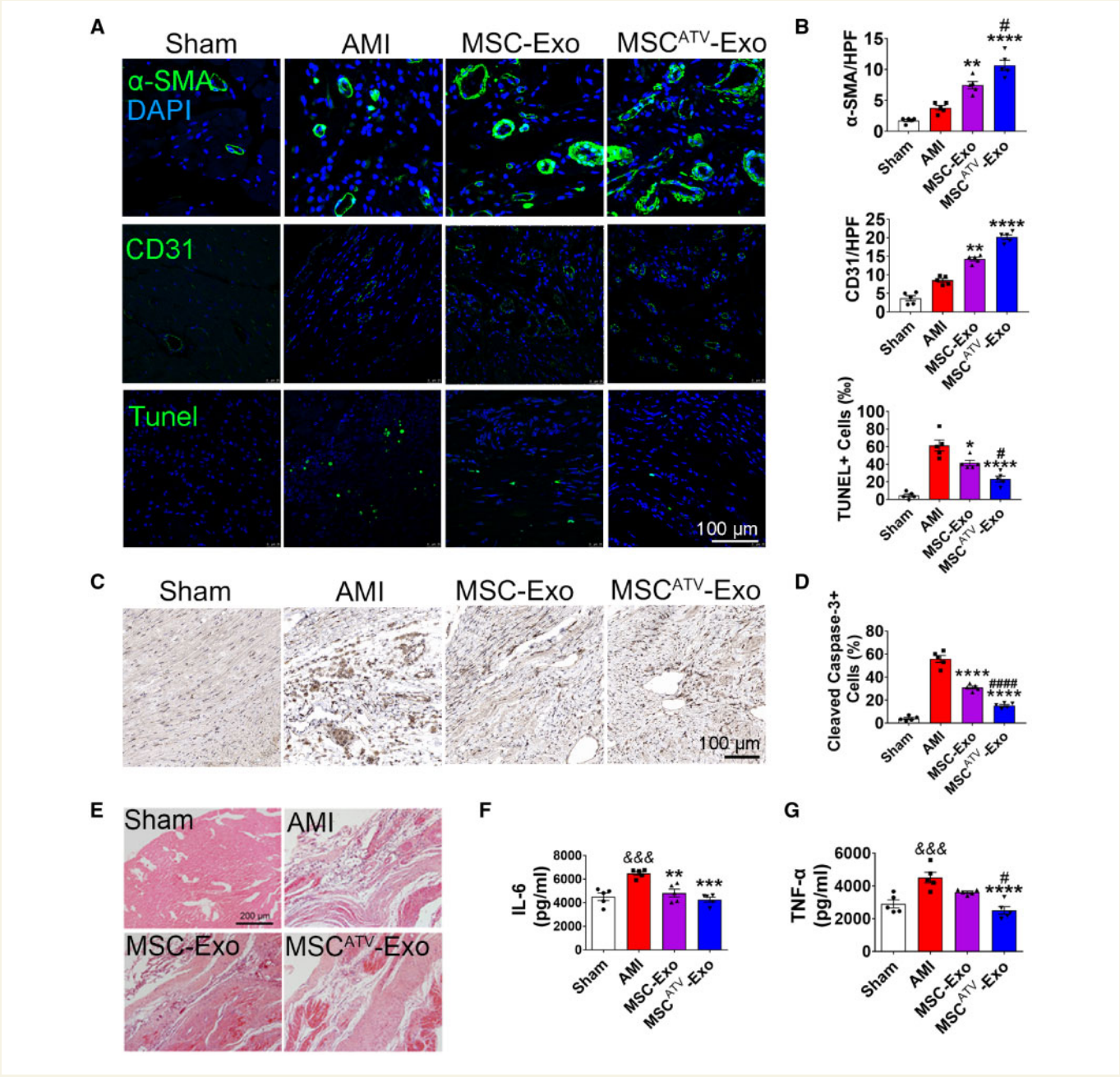


**Figure 5** MSC$^{ATV}$-Exo promoted angiogenesis and reduced cardiac apoptosis and inflammation after infarction. (*A*) Neovascularization at the border zone on Day 28 post-MI was identified by staining with α-SMA and CD31 (green) and nuclei (blue). TUNEL staining at the border zone on Day 28 post-MI with TUNEL (green) and nuclei (blue). Scale bar =100 μm. (*B*) Quantification of α-SMA+ cells, CD31+ cells and TUNEL+ cells in A ($n = 5$). (*C*) Cleaved Caspase-3 staining at the border zone on Day 28 post-MI. Scale bar =100 μm. (*D*) Quantification of Cleaved Caspase-3+ cells in C ($n = 5$). Apoptosis rate was quantified as the percentage of cells that were positive for TUNEL and Cleaved Caspase-3 staining. (*E*) HE staining at the border zone on Day 28 after MI. Scale bar =200 μm. (*F* and *G*) Quantification of IL-6 and TNF-α expression level in the infarct border zone tissue of rat heats using ELISA method ($n = 5$). All data are mean ± SEM. Statistical analysis was performed with one-way ANOVA followed by Tukey's test. $^{\&\&}P < 0.01$, $^{\&\&\&}P < 0.001$ vs. Sham or Control group; $^{*}P < 0.05$, $^{**}P < 0.01$, $^{***}P < 0.001$, $^{****}P < 0.0001$ vs. AMI group; $^{\#}P < 0.05$, $^{\#\#}P < 0.01$, $^{\#\#\#}P < 0.001$, $^{\#\#\#\#}P < 0.0001$ vs. MSC-Exo group.

exosomes was established by Agilent 2200 TapeStation Instrument and was showed in Supplementary material online,*Figure S6*. In total, 450 lncRNAs were identified to be upregulated (over 1.5-fold change) in MSC$^{ATV}$-Exo compared to MSC-Exo (*Figure 6A* and *B* and Supplementary material online, *Table S2*). However, most of these lncRNAs have not been functionally characterized, such as LOC108350691, LOC102551940, ENSRNOG00000024294, and LOC108352067. Among the remaining candidate lncRNA, such as Mall, Ftx, Mroh2a, Skint10, and Thumpd3-as1, none of them have been reported to be involved in cardiovascular cellular function regulation, so we focused on lncRNA H19, expression of which has been previously shown to be associated with exosome-mediated angiogenesis and cardiovascular disease regulation.[34–38] The Reads of RNA-seq of the exosomes samples covered the whole length of lncRNA H19 sequence (Supplementary material online, *Figure*

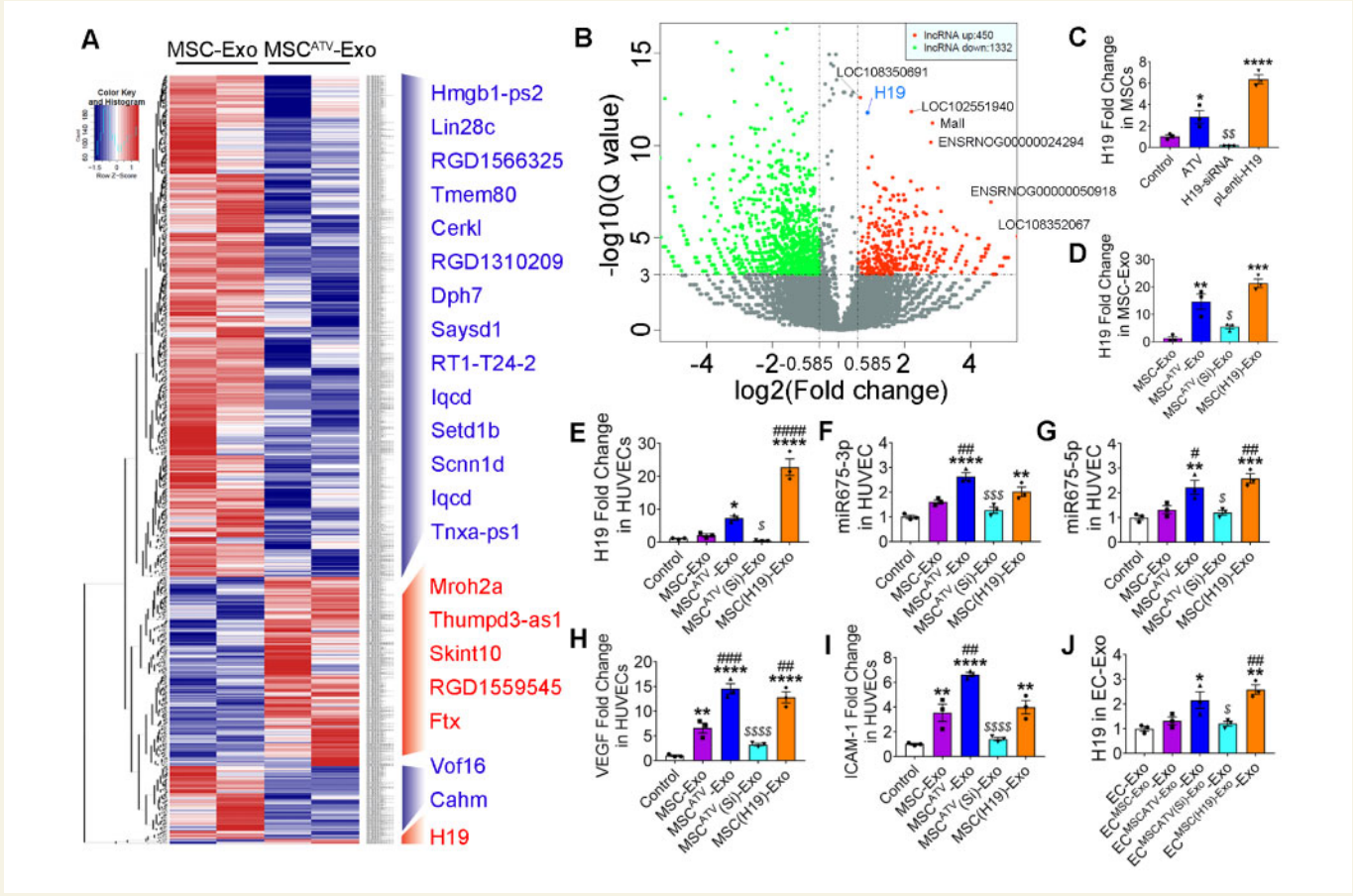


**Figure 6** Exosomal lncRNA expression in MSC-Exo and MSC$^{ATV}$-Exo. (*A*) Heat map based on raw lncRNA expression values (blue represents low expression and red represent high expression) with two-way hierarchical clustering. (*B*) Volcano plot showing log2 (Fold change) (MSC$^{ATV}$-Exo vs. MSC-Exo) on the *x*-axis and -log10(Q value) on the *y*-axis. lncRNA H19 indicated in blue was significantly increased in MSC$^{ATV}$-Exo after correction for multiple comparisons. $n = 2$. (*C* and *D*) Expression values for lncRNA H19 in MSCs treated by PBS, ATV, H19 siRNA, or H19 overexpression lentivirus tested by qRT-PCR (*C*) and exosomes derived from each kind of MSCs (*D*). $n = 3$, $^{*}P < 0.05$, $^{**}P < 0.01$, $^{***}P < 0.001$ vs. Control; $^{\$}P < 0.05$ vs. ATV group. (*E*) Expression values for lncRNA H19 in HUVECs treated by different MSC-Exo (*F* and *G*) qRT-PCR analyses for expression level of miR-675-3p (*F*) and miR-675-5p (*G*) in HUVECs treated with PBS (Control), MSC-Exo, MSC$^{ATV}$-Exo, MSC$^{ATV}$(Si)-Exo, and MSC(H19)-Exo. $n = 3$ for each group. (*H* and *I*) qRT-PCR analyses for VEGF (*H*) and ICAM-1 (*I*) were done on HUVECs 18 h after treatment with PBS (Control), MSC-Exo, MSC$^{ATV}$-Exo, MSC$^{ATV}$(Si)-Exo, and MSC(H19)-Exo. $n = 3$ for each group; $^{*}P < 0.05$, $^{**}P < 0.01$, $^{***}P < 0.001$, $^{****}P < 0.0001$ vs. Control; $^{\#}P < 0.05$, $^{\#\#}P < 0.01$, $^{\#\#\#}P < 0.001$, $^{\#\#\#\#}P < 0.0001$ vs. MSC-Exo group; $^{\$}P < 0.05$, $^{\$\$\$}P < 0.001$, $^{\$\$\$\$}P < 0.0001$ vs. MSC$^{ATV}$-Exo group. (*J*) Expression values for lncRNA H19 in various of MSC-Exo-pretreated HUVECs derived exosomes. $^{*}P < 0.05$, $^{**}P < 0.01$ vs. EC$^{MSC\text{-}Exo}$-Exo group; $^{\#\#}P < 0.01$ vs. EC$^{MSCATV(Si)\text{-}Exo}$-Exo group. All data are mean ± SEM. Statistical analysis was performed with Mann–Whitney *U* test for comparison of two groups and Bonferroni correction in volcano plot for multiplicity correction and one-way ANOVA followed by Tukey's test in qRT-PCR assay.

*S7*). After treating with 1 μmol/L ATV for 24 h, MSCs increased H19 expression almost three-fold as confirmed by the real time-PCR (*Figure 6C*). Moreover, H19 expression level in MSC$^{ATV}$-Exo was about 13-fold higher than that in MSC-Exo (*Figure 6D*). These data suggested that ATV pretreatment increased the expression level of lncRNA H19 in MSCs and its release via exosomes.

## 3.8 LncRNA H19 mediates MSC$^{ATV}$-Exo function on promoting angiogenesis and myocardial injury repair

Based on above-mentioned data, we surmised that lncRNA H19 may function as a mediator of the observed beneficial effects of the MSC$^{ATV}$-Exo. To test our hypothesis, we silenced and overexpressed lncRNA H19 in ATV pretreated or non-treated MSCs (*Figure 6C*), and then derived exosomes from these MSCs (MSC$^{ATV}$(Si)-Exo and MSC(H19)-Exo, *Figure 6D*). No apparent changes in morphological appearance were discovered in the lncRNA H19 knocked down or overexpressed cells. H19 exon1 encodes two conserved microRNAs, miR-675-3p and miR-675-5p, both of which have been implicated in cell differentiation and angiogenesis.[39] In addition, lncRNA H19 together with miR-675-3p and miR-675-5p were reported to regulate the expression of vascular endothelial growth factor (VEGF) and intercellular adhesion molecule-1 (ICAM-1) in HUVEC and cancer cells.[34,40] Interestingly, we found that treating HUVECs with MSC$^{ATV}$-Exo augmented the expression of lncRNA H19, miR-675-3p, and miR-675-5p as well as VEGF and ICAM-1 in HUVECs (*Figure 6E–I*). Consistently, inhibition of H19 led to a significant decrease in the expression of above-mentioned miRNAs and genes

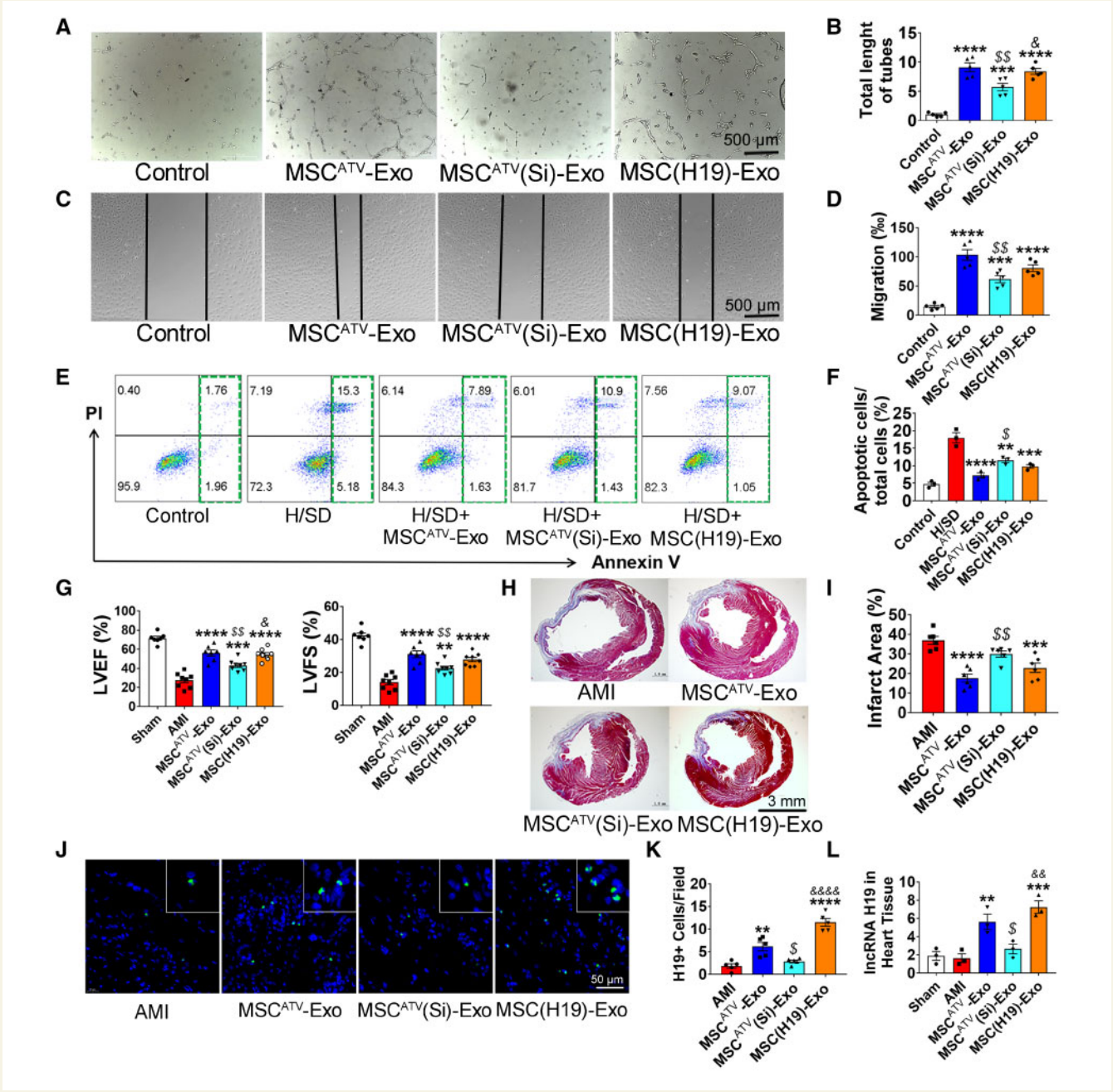


**Figure 7** lncRNA H19 is involved in MSC$^{ATV}$-Exo-mediated biological function of endothelial cells and improvement of myocardial repair. (*A*) Tube formation assay using HUVECs treated with PBS (Control), MSC$^{ATV}$-Exo, MSC$^{ATV}$(Si)-Exo, or MSC(H19)-Exo without FBS for 6 h. (*B*) Quantification of tube length in A ($n = 5$). (*C*) Scratch assay using HUVECs treated with PBS, MSC$^{ATV}$-Exo, MSC$^{ATV}$(Si)-Exo or MSC(H19)-Exo without FBS for 12 h. Scale bar = 500 μm. (*D*) Quantification of migration in C ($n = 5$). (*E*) Scatter diagram of apoptosis in HUVECs treated with negative control, PBS, MSC$^{ATV}$-Exo, MSC$^{ATV}$(Si)-Exo, or MSC(H19)-Exo under H/SD. (*F*) Histogram of apoptosis in different groups ($n = 3$). (*G*) LVEF and LVFE value in rats transplanted with PBS, MSC$^{ATV}$-Exo, MSC$^{ATV}$(Si)-Exo or MSC(H19)-Exo, and sham groups at 4-week post-MI ($n = 8$ for each group). (*H*) Representative transverse heart sections analysed with Masson Trichrome staining at 4 weeks after MI. Red, myocardium; blue, scarred fibrosis. (*I*) Quantitative data for the LV fibrotic area ($n = 6$ for each group). (*J*) H19 positive cells in hearts sections were labelled with a lncRNA-H19 probe (green) using Fluorescent in site hybridization (FISH). Nuclei were counterstained with DAPI. The number of positive cells in the field was quantified. (*K*) H19+ cells Quantification results in *J* ($n = 5$). (*L*) qRT-PCR analyses for expression level of lncRNA H19 in PBS, MSC$^{ATV}$-Exo, MSC$^{ATV}$(Si)-Exo, or MSC(H19)-Exo transplanted heart tissue as well as sham group. $^{*}P < 0.05$, $^{**}P < 0.01$, $^{***}P < 0.001$, $^{****}P < 0.0001$ vs. Control or H/SD or AMI group; $^{\$}P < 0.05$, $^{\$\$}P < 0.01$ vs. MSC$^{ATV}$-Exo group; $^{\&}P < 0.05$, $^{\&\&}P < 0.01$, $^{\&\&\&\&}P < 0.0001$ vs. MSC$^{ATV}$(Si)-Exo group. All data are mean ± SEM. Statistical analysis was performed with one-way ANOVA followed by Tukey's test.

and overexpressing H19 mimicked the effects of $MSC^{ATV}$-Exo treatment group (*Figure 6E–I*). As EC-Exo mediated the protective effects of $MSC^{ATV}$-Exo on cardiomyocytes (*Figure 3*), we also tested the expression of lncRNA H19 in exosomes derived from MSC-Exo-pretreated HUVECs. Intriguingly, a significantly higher level of lncRNA H19 (about two-fold), though relatively low, was still detectable in $EC^{MSCATV\text{-}Exo}$-Exo and $EC^{MSC(H19)\text{-}Exo}$-Exo compared to $EC^{MSC\text{-}Exo}$-Exo and EC-Exo control (*Figure 6J*).

We then further explored the effects of H19 silencing and overexpression on EC function. $MSC^{ATV}$(Si)-Exo failed to improve angiogenesis (*Figure 7A* and *B*) and cell migration (*Figure 7C* and *D*) on HUVECs. H19 silencing also abrogated $MSC^{ATV}$-Exo-mediated anti-apoptosis effect on HUVECs (*Figure 7E* and *F*). In contrast, MSC(H19)-Exo can simulate the pro-angiogenesis and anti-apoptosis effects of $MSC^{ATV}$-Exo on HUVECs (*Figure 7A–F*).

To explore if lncRNA H19 mediates $MSC^{ATV}$-Exo's beneficial effects on *in vivo* heart function improvement, we delivered $MSC^{ATV}$-Exo, $MSC^{ATV}$(Si)-Exo and MSC(H19)-Exo into acutely infarcted rat hearts. LVEF were evaluated at 4 weeks after indicated treatments. $MSC^{ATV}$(Si)-Exo groups showed significantly lower and MSC(H19)-Exo groups showed similar level of LVEF and LVFS at fourth-week post-MI compared to $MSC^{ATV}$-Exo group (*Figure 7G*). Infarct size in animals treated with $MSC^{ATV}$(Si)-Exo failed to be reduced compared to those treated with $MSC^{ATV}$-Exo and MSC(H19)-Exo (*Figure 7H* and *I*). Moreover, we detected the lncRNA H19 expression in the treated hearts by using lncRNA FISH and qPCR. The results showed that H19 was significantly increased in both $MSC^{ATV}$-Exo and MSC(H19)-Exo groups and decreased in $MSC^{ATV}$(Si)-Exo-treated hearts (*Figure 7J–L*). Taken together, these results indicated that $MSC^{ATV}$-Exo positively regulate angiogenesis and myocardial injury repair at least partially through lncRNA H19, and H19 can be transferred to the infarcted hearts through $MSC^{ATV}$-Exo transplantation.

## 4. Discussion

Stem-cell therapy was previously considered to regenerate injured heart by replenishing new cardiomyocytes through replication and then differentiation. However, recent studies indicated that MSCs achieved their cardioprotective effect mainly through secreting paracrine factors including exosomes.[8,9] Over the past few years, exosomes derived from MSCs have been shown to reduce myocardial ischaemia injury and improve cardiac function after MI, suggesting that exosome-based approaches hold great promise as a potential novel cell-free therapy for cardiac repair.[14,41,42] Results described here indicated that (i) $MSC^{ATV}$-Exo promoted ECs tube-like structure formation, migration, and inhibited ECs apoptosis under H/SD condition; (ii) ECs mediated the protective benefit of $MSC^{ATV}$-Exo on CMs under H/SD; (iii) $MSC^{ATV}$-Exo showed a higher efficiency in improving cardiac function and reducing fibrosis of AMI rat hearts; and (iv) the beneficial effect of $MSC^{ATV}$-Exo might be partially mediated by lncRNA H19 that could be secreted to ECs via exosomes to stimulate angiogenesis in peri-infarct region (*Figure 8*). To the best of our knowledge, this is the first study that investigated a pro-cardioprotective effect of ATV on MSC-derived exosomes.

Compared with stem cell transplantation therapy, exosome treatment for MI have yielded similar results and showed the advantages of no teratoma formation, low tumorigenic potential, and minimal immunogenicity. However, successful exosome therapeutics for myocardial repair will require much more extensive testing and validation to ensure their safety and improve their efficacy. In recent years, there has been significant effort to develop modified stem cells-derived exosomes that could bring superior effect on repairing the infarcted heart. Yu *et al.*[43] demonstrated that exosomes derived from GATA4-overexpressing MSCs were enriched in anti-apoptotic miRNAs and when injected into rat MI model conferred cardioprotective effects. Another recent study by Ma *et al.*[44] demonstrated that exosomes obtained from Akt-modified human umbilical cord MSCs had the ability to augment cardiac regeneration and promoted angiogenesis via activating platelet-derived growth factor D. Although these genetic approaches appear to be effective in increasing the expression of specific cytokine or microRNA in MSC-Exo, currently, they are still infeasible in clinical practice. Instead, our approach of pre-treating MSCs with ATV is more straightforward and clinically feasible. Therefore, our findings may result in immediate translational implications for the treatment of AMI patients. To our knowledge, there has been limited studies that explored this kind of effect with commonly used medications.

In addition, heart function improvement is the main goal of cardiac regeneration medicine and the major factor related to the outcome of therapies in both preclinical and clinical studies. Compared to only modest benefit was found in heart function (LVEF improved 2–5%) after MSCs transplantation in clinical trials, preclinical studies about MSC exosomes therapy reported a significant improvement in heart function (LVEF improved 10–15%) and a superior augment in genetic modified exosomes (LVEF improved 20–25%).[7,43,44] Consistently, we also realized an improvement of heart function after AMI in both MSC-Exo and $MSC^{ATV}$-Exo-treated groups, in which LVEF modestly increased 11% and remarkably elevated 27% separately (*Table 1*). Thus, our strategy of ATV pretreatment is comparable or even better in heart function recovery compared with current reported gene modified methods.

Angiogenesis is a process of developing new blood vessels from the existing vessels. Stimulating angiogenesis in the infarct area can help salvage myocardium by clearing apoptotic cells, decreasing scar tissue, and recruiting progenitor cells for tissue regeneration.[45] Recent studies demonstrated that exosomes isolated from stem cells, such as MSCs, CPCs, ESC, and CD34+ stem cells can stimulate angiogenesis both *in vitro* and *in vivo*.[41,46–49] Consistently, we also found MSC-derived exosomes promoted angiogenesis and stimulated anti-apoptosis ability of ECs. Moreover, ATV-pretreated MSC-derived exosomes showed a greater angiogenic potential compared to non-pretreated MSC-Exo (*Figure 2*). Together with the facts that various kinds of vascular active factors have been found in exosomes and ECs have an efficient ability to uptake the MSC-Exo, angiogenesis could be a common and key function of stem cells derived exosomes.

Some early studies showed that CMs can internalize PKH26 labelled exosomes after incubation for 12 or 24 h,[17,46] but barely any study has examined the internalization mode of CMs during first several hours and performed the head to head comparison with ECs and fibroblasts. We found that CMs uptake MSC-Exo very inefficiently compared to ECs and fibroblasts in the first 2 h and even in 12 h. (*Figure 1D*). Consistent with our findings, Yu *et al.*[43] investigated the mode of PKH26 labelled exosomes delivery to CM using a time-lapse imaging system. They found that no clear exosomes could be detected in CMs during the first 2 h and negligible red fluorescent spots indicating exosomes appeared in CMs by Hour 3. In contrast, we found that H9C2 cardiomyocytes uptake much more PKH26 labelled EC-Exo in 12 h compared to MSC-Exo (*Figures 3C and 1D*). The mechanism for this is unclear, but may relate in part to the connexins and integrins embedded in the exosomal membranes from different cell types.[50,51] Such kind of delivery mode of exosomes to CMs is important for their function. In this study, we

investigated the effect of MSC-derived exosomes on CMs under H/SD and found that no significant anti-apoptosis effect was observed by incubation of CMs directly with $MSC^{ATV}$-Exo, while exosomes derived from ECs treated with $MSC^{ATV}$-Exo conferred beneficial effect on H9C2 cardiomyocytes challenged with H/SD. These results demonstrated that exosome uptake efficiency varies from cell to cell and clinical application of therapeutic exosomes may rely on an in-depth understanding of the mechanism of uptake and action to fully harness their beneficial effects.

It is well known that exosomes contain proteins, mRNAs, miRNAs, etc., which can be transferred to cells to regulate intracellular signalling pathways in the recipient cells.[45,52] In recent years, increasing evidence suggested that exosomal lncRNAs mediate the effect of exosomes on many biological processes.[32] However, the role of the lncRNAs contained in stem cell-derived exosomes played in cardiovascular repair has remained unexplored. In this study, expression profile of lncRNA in ATV-pretreated MSC-derived exosomes revealed that lncRNA H19 was significantly higher in $MSC^{ATV}$-Exo than in MSC-Exo. Moreover, the expression level of miR-675-5p and miR-675-3p encoded by lncRNA H19 exon 1 as well as H19 itself was also increased in ECs upon treatment with $MSC^{ATV}$-Exo. Of note, H19 level in EC-Exo and the infarcted hearts also can be elevated by $MSC^{ATV}$-Exo treatment. These results showed that the level of increased expression of H19 in $MSC^{ATV}$-Exo, $EC^{MSCATV\text{-}Exo}$, $EC^{MSCATV\text{-}Exo}$-Exo and infarcted hearts gradually reduced from about 13-fold to seven-fold and ended up with about two- to three-fold compared to non-treated groups, which indicates the efficiency of H19 transfer from ATV treated MSC to hearts tissue in the mediation of ECs and EC-Exo (*Figures 6C–E, J and 7L*).

The lncRNA H19, a 2.3 kb lncRNA transcribed from the H19 gene, is highly expressed in several tissues of foetus, but the expression is significantly reduced after birth.[53,54] MiR-675 is found to be embedded in H19's first exon and both of the H19 lncRNA exon structure and miR-675 are conserved between rodents and humans.[55] Researchers have reported multiple functions of H19 in cancer and cardiovascular diseases as well as its diverse downstream pathway mechanisms in the target cells, such as lncRNA H19/miR-675 axis, HIF1α/Mdm2-p53, NOTCH1, and STAT3/p21 pathway.[36–38,53] Recently, it has been reported that lncRNA H19 is an essential regulator of endothelial senescence and promotes proliferation in endothelial cells.[38,56] In addition, recent study demonstrated that CD90+ liver cancer cells modulate phenotype of ECs and promote angiogenesis through exosome-contained H19 lncRNA. The mRNA levels of the proangiogenic factor VEGF and intercellular adhesion molecules ICAM-1 also increased in ECs after exosome treatment.[34] In this study, we examined the expression level of VEGF and ICAM-1 in ECs treated by various kinds of MSC-derived exosomes, and found a significantly higher level of VEGF and ICAM-1 expression as well as miR-675 in $MSC^{ATV}$-Exo and MSC(H19)-Exo treating groups than in MSC-Exo and $MSC^{ATV}$(Si)-Exo treating groups (*Figure 6H* and *I*). Based on these and other observation, we propose that lncRNA H19/miR-675 axis mediated the effect of $MSC^{ATV}$-Exo in promoting angiogenesis and endothelial survival through regulating proangiogenic factors. The promotion of EC function *in vitro* and cardiac protection *in vivo* induced by $MSC^{ATV}$-Exo was markedly abolished when lncRNA H19 expression in MSCs was silenced and can be mimicked by overexpressing H19 in MSCs, supporting that exosomal lncRNA H19 targeting on functional regulation on ECs plays an important role in $MSC^{ATV}$-Exo-mediated cardiovascular protection.

Aging is a major independent risk factor for the progress of cardiovascular disease.[29,30] Aging leads to cellular senescence and increased inflammatory activation which result in thickened intima, increased arterial stiffness, endothelial dysfunction, and chronic vascular inflammation.[57] Recent studies showed that lncRNA H19 is expressed in the adult endothelium, valve interstitial cells, and aortic smooth muscle cells (SMCs) and is decreased during aging.[36–38] Of note, H19 depletion in ECs led to cellular senescence and dysfunction while overexpression of H19 ameliorates endothelial function in aged aortas.[38] In this study, we also investigated the level of cellular senescence marker in the hearts after exosomes therapy. Interestingly, although a significant increase of senescent cells (4–8%) was found in all of the infarcted groups, no significant difference was found among MSC-Exo, $MSC^{ATV}$-Exo and AMI groups (Supplementary material online,*Figure S5*). Therefore, here, we did not observe the effects of elevated H19 on the senescence of the infarcted hearts which may due to the acute course of AMI mainly leading to cell necrosis and apoptosis. Nevertheless, further investigations on the role of H19 contained in $MSC^{ATV}$-Exo during the process of aging cardiovascular diseases, such as calcific aortic valve disease, aortic aneurysm and atherosclerosis, are still needed in the future studies.

A successful exosome therapeutic regimen for cardiac repair would likely elicit a combination of beneficial effects capable of attenuating cardiac fibrosis, promoting angiogenesis and improving cardiac function. Although $MSC^{ATV}$-Exo showed a much-improved therapeutic effects compared to MSC-Exo, further preclinical studies are required to validate its efficacy and safety before this strategy could move forward as potential cell-free therapeutics for myocardial repair. On the other hand, successful cardiac repair post-MI requires tissue regeneration in order to restore cardiac function and decrease LV remodelling. Combined treatment of $MSC^{ATV}$-Exo with cardiomyocyte inducible stem cells or loading exosomes with cell fate reprogramming factors could be prospective strategies to achieve this goal.

## 5. Conclusions

ATV pretreatment promotes the function of MSC-derived exosome in enhancing angiogenesis, protecting cardiomyocytes and improving cardiac function after infarction. LncRNA H19 and its downstream signalling pathways mediate the cardioprotective effects of $MSC^{ATV}$-Exo angiogenesis.

## Supplementary material

Supplementary material is available at *Cardiovascular Research* online.


## Acknowledgements

We thank Drs Yang Zhou and Jiandong Liu at the University of North Carolina at Chapel Hill for their scientific advices. We also thank Peihe Wang in the Experimental Animal Center of Fuwai Hospital and Qing Xu of Central Laboratory of Capital University of Medical Sciences for their technical assistance.

**Conflict of interest:** none declared.

## Funding

This work was supported by the CAMS Innovation Fund for Medical Sciences (CIFMS, 2016-12M-1-009), Innovative Research Foundation of Peking Union Medical College (2016-1002-01-03), grants from National

Natural Science Foundation of China (81370223, 81573957 and 81670337), National Science and Technology Major Project of the Ministry of Science and Technology of China (2014ZX09101042001), and the programme of China Scholarships Council (No. 201706210393).

## References


1. GBD 2016 Mortality Collaborators. Global, regional, and national under-5 mortality, adult mortality, age-specific mortality, and life expectancy, 1970-2016: a systematic analysis for the Global Burden of Disease Study 2016. *Lancet* 2017;**390**:1084–1150.
2. GBD 2016 Mortality Collaborators. Global, regional, and national age-sex specific mortality for 264 causes of death, 1980–2016: a systematic analysis for the Global Burden of Disease Study 2016. *Lancet* 2017;**390**:1151–1210.
3. Orlic D, Kajstura J, Chimenti S, Jakoniuk I, Anderson SM, Li B, Pickel J, McKay R, Nadal-Ginard B, Bodine DM, Leri A, Anversa P. Bone marrow cells regenerate infarcted myocardium. *Nature* 2001;**410**:701–705.
4. Williams AR, Hatzistergos KE, Addicott B, McCall F, Carvalho D, Suncion V, Morales AR, Da SJ, Sussman MA, Heldman AW, Hare JM. Enhanced effect of combining human cardiac stem cells and bone marrow mesenchymal stem cells to reduce infarct size and to restore cardiac function after myocardial infarction. *Circulation* 2013;**127**:213–223.
5. Lee CY, Kim R, Ham O, Lee J, Kim P, Lee S, Oh S, Lee H, Lee M, Kim J, Chang W. Therapeutic potential of stem cells strategy for cardiovascular diseases. *Stem Cells Int* 2016;**2016**:1.
6. Fisher SA, Doree C, Mathur A, Martin-Rendon E. Meta-analysis of cell therapy trials for patients with heart failure. *Circ Res* 2015;**116**:1361–1377.
7. Afzal MR, Samanta A, Shah ZI, Jeevanantham V, Abdel-Latif A, Zuba-Surma EK, Dawn B. Adult bone marrow cell therapy for ischemic heart disease: evidence and insights from randomized controlled trials. *Circ Res* 2015;**117**:558–575.
8. Makridakis M, Roubelakis MG, Vlahou A. Stem cells: insights into the secretome. *Biochim Biophys Acta* 2013;**1834**:2380–2384.
9. Gnecchi M, Zhang Z, Ni A, Dzau VJ. Paracrine mechanisms in adult stem cell signaling and therapy. *Circ Res* 2008;**103**:1204–1219.
10. Haider H, Jiang S, Idris NM, Ashraf MI. 1-overexpressing mesenchymal stem cells accelerate bone marrow stem cell mobilization via paracrine activation of SDF-1alpha/CXCR4 signaling to promote myocardial repair. *Circ Res* 2008;**103**:1300–1308.
11. Tang J, Wang J, Guo L, Kong X, Yang J, Zheng F, Zhang L, Huang Y. Mesenchymal stem cells modified with stromal cell-derived factor 1 alpha improve cardiac remodeling via paracrine activation of hepatocyte growth factor in a rat model of myocardial infarction. *Mol Cells* 2010;**29**:9–19.
12. Marote A, Teixeira FG, Mendes-Pinheiro B, Salgado AJ. MSCs-derived exosomes: cell-secreted nanovesicles with regenerative potential. *Front Pharmacol* 2016;**7**:231.
13. Huang P, Tian X, Li Q, Yang Y. New strategies for improving stem cell therapy in ischemic heart disease. *Heart Fail Rev* 2016;**21**:737–752.
14. Lai RC, Arslan F, Lee MM, Sze NS, Choo A, Chen TS, Salto-Tellez M, Timmers L, Lee CN, El OR, Pasterkamp G, de Kleijn DP, Lim SK. Exosome secreted by MSC reduces myocardial ischemia/reperfusion injury. *Stem Cell Res* 2010;**4**:214–222.
15. Lamichhane TN, Sokic S, Schardt JS, Raiker RS, Lin JW, Jay SM. Emerging roles for extracellular vesicles in tissue engineering and regenerative medicine. *Tissue Eng Part B Rev* 2015;**21**:45–54.
16. Barile L, Moccetti T, Marban E, Vassalli G. Roles of exosomes in cardioprotection. *Eur Heart J* 2017;**38**:1372–1379.
17. Zhu J, Lu K, Zhang N, Zhao Y, Ma Q, Shen J, Lin Y, Xiang P, Tang Y, Hu X, Chen J, Zhu W, Webster KA, Wang J, Yu H. Myocardial reparative functions of exosomes from mesenchymal stem cells are enhanced by hypoxia treatment of the cells via transferring microRNA-210 in an nSMase2-dependent way. *Artif Cells Nanomed Biotechnol* 2018;**46**:1659–1670.
18. Gray WD, French KM, Ghosh-Choudhary S, Maxwell JT, Brown ME, Platt MO, Searles CD, Davis ME. Identification of therapeutic covariant microRNA clusters in hypoxia-treated cardiac progenitor cell exosomes using systems biology. *Circ Res* 2015;**116**:225–263.
19. Yang YJ, Qian HY, Huang J, Geng YJ, Gao RL, Dou KF, Yang GS, Li JJ, Shen R, He ZX, Lu MJ, Zhao SH. Atorvastatin treatment improves survival and effects of implanted mesenchymal stem cells in post-infarct swine hearts. *Eur Heart J* 2008;**29**:1578–1590.
20. Song L, Yang Y, Dong Q, Qian H, Gao R, Qiao S, Shen R, He Z, Lu M, Zhao S, Geng Y, Gersh BJ. Atorvastatin enhance efficacy of mesenchymal stem cells treatment for swine myocardial infarction via activation of nitric oxide synthase. *PLoS One* 2013;**8**:e65702.
21. Xu H, Yang Y, Yang T, Qian H. Statins and stem cell modulation. *Ageing Res Rev* 2013;**12**:1–7.
22. Li N, Yang YJ, Qian HY, Li Q, Zhang Q, Li XD, Dong QT, Xu H, Song L, Zhang H. Intravenous administration of atorvastatin-pretreated mesenchymal stem cells improves cardiac performance after acute myocardial infarction: role of CXCR4. *Am J Transl Res* 2015;**7**:1058–1070.
23. Tamboli IY, Barth E, Christian L, Siepmann M, Kumar S, Singh S, Tolksdorf K, Heneka MT, Lutjohann D, Wunderlich P, Walter J. Statins promote the degradation of extracellular amyloid-peptide by microglia via stimulation of exosome-associated insulin-degrading enzyme (IDE) secretion. *J Biol Chem* 2010;**285**:37405–37414.
24. Luo L, Tang J, Nishi K, Yan C, Dinh P, Cores J, Kudo T, Zhang J, Li TS, Cheng K. Fabrication of synthetic mesenchymal stem cells for the treatment of acute myocardial infarction in mice. *Circ Res* 2017;**120**:1768–1775.
25. Tang J, Shen D, Caranasos TG, Wang Z, Vandergriff AC, Allen TA, Hensley MT, Dinh PU, Cores J, Li TS, Zhang J, Kan Q, Cheng K. Therapeutic microparticles functionalized with biomimetic cardiac stem cell membranes and secretome. *Nat Commun* 2017;**8**:13724.
26. Thery C, Amigorena S, Raposo G, Clayton A. Isolation and characterization of exosomes from cell culture supernatants and biological fluids. *Curr Protoc Cell Biol* 2006; Chapter 3:Unit 3.22.
27. Li Q, Dong QT, Yang YJ, Tian XQ, Jin C, Huang PS, Jiang LP, Chen GH. AMPK-mediated cardioprotection of atorvastatin relates to the reduction of apoptosis and activation of autophagy in infarcted rat hearts. *Am J Transl Res* 2016;**8**:4160–4171.
28. Yuyama K, Sun H, Mitsutake S, Igarashi Y. Sphingolipid-modulated exosome secretion promotes clearance of amyloid-beta by microglia. *J Biol Chem* 2012;**287**:10977–10989.
29. Dutta D, Calvani R, Bernabei R, Leeuwenburgh C, Marzetti E. Contribution of impaired mitochondrial autophagy to cardiac aging: mechanisms and therapeutic opportunities. *Circ Res* 2012;**110**:1125–1138.
30. Lewis-McDougall FC, Ruchaya PJ, Domenjo-Vila E, Shin TT, Prata L, Cottle BJ, Clark JE, Punjabi PP, Awad W, Torella D, Tchkonia T, Kirkland JL, Ellison-Hughes GM. Aged-senescent cells contribute to impaired heart regeneration. *Aging Cell* 2019;**18**:e12931.
31. Baker DJ, Wijshake T, Tchkonia T, LeBrasseur NK, Childs BG, van de Sluis B, Kirkland JL, van Deursen JM. Clearance of p16Ink4a-positive senescent cells delays ageing-associated disorders. *Nature* 2011;**479**:232–236.
32. Gezer U, Ozgur E, Cetinkaya M, Isin M, Dalay N. Long non-coding RNAs with low expression levels in cells are enriched in secreted exosomes. *Cell Biol Int* 2014;**38**:1076–1079.
33. Takahashi K, Yan IK, Kogure T, Haga H, Patel T. Extracellular vesicle-mediated transfer of long non-coding RNA ROR modulates chemosensitivity in human hepatocellular cancer. *FEBS Open Bio* 2014;**4**:458–467.
34. Conigliaro A, Costa V, Lo DA, Saieva L, Buccheri S, Dieli F, Manno M, Raccosta S, Mancone C, Tripodi M, De Leo G, Alessandro R. CD90+ liver cancer cells modulate endothelial cell phenotype through the release of exosomes containing H19 lncRNA. *Mol Cancer* 2015;**14**:155.
35. Gong LC, Xu HM, Guo GL, Zhang T, Shi JW, Chang C. Long non-coding RNA H19 protects H9c2 cells against hypoxia-induced injury by targeting microRNA-139. *Cell Physiol Biochem* 2017;**44**:857–869.
36. Hadji F, Boulanger M-C, Guay S-P, Gaudreault N, Amellah S, Mkannez G, Bouchareb R, Marchand JT, Nsaibia MJ, Guauque-Olarte S, Pibarot P, Bouchard L, Bossé Y, Mathieu P. Altered DNA methylation of long noncoding RNA H19 in calcific aortic valve disease promotes mineralization by silencing NOTCH1. *Circulation* 2016;**134**:1848–1862.
37. Li DY, Busch A, Jin H, Chernogubova E, Pelisek J, Karlsson J, Sennblad B, Liu S, Lao S, Hofmann P, Backlund A, Eken SM, Roy J, Eriksson P, Dacken B, Ramanujam D, Dueck A, Engelhardt S, Boon RA, Eckstein HH, Spin JM, Tsao PS, Maegdefessel L. H19 induces abdominal aortic aneurysm development and progression. *Circulation* 2018;**138**:1551–1568.
38. Hofmann P, Sommer J, Theodorou K, Kirchhof L, Fischer A, Li Y, Perisic L, Hedin U, Maegdefessel L, Dimmeler S, Boon RA. Long non-coding RNA H19 regulates endothelial cell aging via inhibition of STAT3 signalling. *Cardiovasc Res* 2019;**115**:230–242.
39. Dey BK, Pfeifer K, Dutta A. The H19 long noncoding RNA gives rise to microRNAs miR-675-3p and miR-675-5p to promote skeletal muscle differentiation and regeneration. *Genes Dev* 2014;**28**:491–501.
40. He P, Zhang Z, Huang G, Wang H, Xu D, Liao W, Kang Y. miR-141 modulates osteoblastic cell proliferation by regulating the target gene of lncRNA H19 and lncRNA H19-derived miR-675. *Am J Transl Res* 2016;**8**:1780–1788.
41. Bian S, Zhang L, Duan L, Wang X, Min Y, Yu H. Extracellular vesicles derived from human bone marrow mesenchymal stem cells promote angiogenesis in a rat myocardial infarction model. *J Mol Med* 2014;**92**:387–397.
42. Lee C, Mitsialis SA, Aslam M, Vitali SH, Vergadi E, Konstantinou G, Sdrimas K, Fernandez-Gonzalez A, Kourembanas S. Exosomes mediate the cytoprotective action of mesenchymal stromal cells on hypoxia-induced pulmonary hypertension. *Circulation* 2012;**126**:2601–2611.
43. Yu B, Kim HW, Gong M, Wang J, Millard RW, Wang Y, Ashraf M, Xu M. Exosomes secreted from GATA-4 overexpressing mesenchymal stem cells serve as a reservoir of anti-apoptotic microRNAs for cardioprotection. *Int J Cardiol* 2015;**182**:349–360.
44. Ma J, Zhao Y, Sun L, Sun X, Zhao X, Sun X, Qian H, Xu W, Zhu W. Exosomes derived from Akt-modified human umbilical cord mesenchymal stem cells improve cardiac regeneration and promote angiogenesis via activating platelet-derived growth factor D. *Stem Cells Transl Med* 2017;**6**:51–59.
45. Dougherty JA, Mergaye M, Kumar N, Chen CA, Angelos MG, Khan M. Potential role of exosomes in mending a broken heart: nanoshuttles propelling future clinical therapeutics forward. *Stem Cells Int* 2017;**2017**:5785436.
46. Barile L, Lionetti V, Cervio E, Matteucci M, Gherghiceanu M, Popescu LM, Torre T, Siclari F, Moccetti T, Vassalli G. Extracellular vesicles from human cardiac progenitor cells inhibit cardiomyocyte apoptosis and improve cardiac function after myocardial infarction. *Cardiovasc Res* 2014;**103**:530–541.

47. Gong M, Yu B, Wang J, Wang Y, Liu M, Paul C, Millard RW, Xiao DS, Ashraf M, Xu M. Mesenchymal stem cells release exosomes that transfer miRNAs to endothelial cells and promote angiogenesis. *Oncotarget* 2017;**8**:45200–45212.
48. Mathiyalagan P, Liang Y, Kim D, Misener S, Thorne T, Kamide CE, Klyachko E, Losordo DW, Hajjar RJ, Sahoo S. Angiogenic mechanisms of human CD34(+) stem cell exosomes in the repair of ischemic hindlimb. *Circ Res* 2017;**120**:1466–1476.
49. Khan M, Nickoloff E, Abramova T, Johnson J, Verma SK, Krishnamurthy P, Mackie AR, Vaughan E, Garikipati VN, Benedict C, Ramirez V, Lambers E, Ito A, Gao E, Misener S, Luongo T, Elrod J, Qin G, Houser SR, Koch WJ, Kishore R. Embryonic stem cell-derived exosomes promote endogenous repair mechanisms and enhance cardiac function following myocardial infarction. *Circ Res* 2015;**117**:52–64.
50. Hoshino A, Costa-Silva B, Shen T, Rodrigues G, Hashimoto A, Tesic Mark M, Molina H, Kohsaka S, Di Giannatale A, Ceder S, Singh S, Williams C, Soplop N, Uryu K, Pharmer L, King T, Bojmar L, Davies AE, Ararso Y, Zhang T, Zhang H, Hernandez J, Weiss JM, Dumont-Cole VD, Kramer K, Wexler LH, Narendran A, Schwartz GK, Healey JH, Sandstrom P, Jørgen Labori K, Kure EH, Grandgenett PM, Hollingsworth MA, de Sousa M, Kaur S, Jain M, Mallya K, Batra SK, Jarnagin WR, Brady MS, Fodstad O, Muller V, Pantel K, Minn AJ, Bissell MJ, Garcia BA, Kang Y, Rajasekhar VK, Ghajar CM, Matei I, Peinado H, Bromberg J, Lyden D. Tumour exosome integrins determine organotropic metastasis. *Nature* 2015;**527**:329–335.
51. Shimaoka M, Kawamoto E, Gaowa A, Okamoto T, Park EJ. Connexins and integrins in exosomes. *Cancers (Basel)* 2019;**11**:106.
52. Zhao J, Li X, Hu J, Chen F, Qiao S, Sun X, Gao L, Xie J, Xu B. Mesenchymal stromal cell-derived exosomes attenuate myocardial ischemia-reperfusion injury through miR-182-regulated macrophage polarization. *Cardiovasc Res* 2019;**115**:1205–1216
53. Gabory A, Ripoche MA, Yoshimizu T, Dandolo L. The H19 gene: regulation and function of a non-coding RNA. *Cytogenet Genome Res* 2006;**113**:188–193.
54. Li H, Yu B, Li J, Su L, Yan M, Zhu Z, Liu B. Overexpression of lncRNA H19 enhances carcinogenesis and metastasis of gastric cancer. *Oncotarget* 2014;**5**:2318–2329.
55. Smits G, Mungall AJ, Griffiths-Jones S, Smith P, Beury D, Matthews L, Rogers J, Pask AJ, Shaw G, VandeBerg JL, McCarrey JR, Renfree MB, Reik W, Dunham I. Conservation of the H19 noncoding RNA and H19-IGF2 imprinting mechanism in therians. *Nat Genet* 2008;**40**:971–976.
56. Yan J, Zhang Y, She Q, Li X, Peng L, Wang X, Liu S, Shen X, Zhang W, Dong Y, Lu J, Zhang G. Long noncoding RNA H19/miR-675 axis promotes gastric cancer via FADD/Caspase 8/Caspase 3 signaling pathway. *Cell Physiol Biochem* 2017;**42**:2364–2376.
57. Lakatta EG, Levy D. Arterial and cardiac aging: major shareholders in cardiovascular disease enterprises: part I: aging arteries: a "set up" for vascular disease. *Circulation* 2003;**107**:139–146.

## Translational perspective

Atorvastatin pretreatment is a simple and clinically feasible approach to augment the therapeutic ability of MSCs derived exosomes in acute myocardial infarction. With superior effects on heart function recovery and infarct area reduction, $MSC^{ATV}$-Exo is a promising product that could serve as a potential cell-free therapeutic for myocardial repair. In addition, successful cardiac repair post-MI requires tissue regeneration in order to restore cardiac function and decrease left ventricle remodeling. Therefore, combined treatment of $MSC^{ATV}$-Exo with cardiomyocyte inducible stem cells and loading exosomes with cardiac cell fate reprogramming factors could be prospective strategies to achieve this goal in future clinical practise.